Methane Decomposition Over Activated carbon - Deactivation Study

Dr. Saba A. Ghani
Associate Prof.
Chem. Eng. Dept.
University of Tikrit
bentimran_ra@yahoo.com

Dr. Mohamed A. Al Sarag
Assistant Prof.
Ministry of Higher Education
University of Tikrit
mohatiya1965@gmail. com

Ghassan H. Abdull Razaq
Engineer
Chem. Eng. Dept.
ghassanaldoori@yahoo.com

Sumaya Q. ASe'ed
Engineer
Northern Refineries Company
Ministry of Oil
sumaia_msh@yahoo.com;

ABSTRACT

Methane decomposition over activated carbons was carried out in a fixed bed, quartz flow reactor to produce CO_x free hydrogen. Activated carbon derived from hardwood was used. The effect of gas hourly space velocity in the range of 6-20 L/hr was studied on decomposition.

Kinetics and deactivation study of methane decomposition and surface properties changes before and after reaction was investigated. The physicochemical properties like surface area and SEM for the spent and fresh catalysts were tested in this work and relates to the carbon activity for production of hydrogen.

A reaction order of 1 is obtained for methane decomposition and activation energy is 205 kJ mol/1. The activated carbon shows a high value of sustainability factor (R_0) at all the implied temperatures. Thiele modulus had a value of 1.288 which indicated fair pore diffusional resistance.

INTRODUCTION

Significant attention in the last few years has been focused on using carbons as a catalyst for thermocatalytic decomposition (TCD) of methane. Carbon catalyst offers several advantages over metal catalysts such as (1) low cost, (2) high temperature resistance, (3) tolerance to sulfur and other potentially harmful impurities in the feedstock, (4) production of a marketable byproduct carbon (that could substantially reduce the net cost of hydrogen production), (5) mitigation of overall CO_2 emissions from the process and (6) no metal carbides formed (formation of carbides may complicate the regeneration of metal catalysts), (Hazzim et al, 2009). Among interesting features of TCD of methane by using carbonaceous catalysts are: 1) it can be catalyzed by carbon produced in the process, so an external catalyst would not be required except for the start-up operation, and 2) separation of carbon product from the carbon catalyst is not necessary(La´zaro et al, 2008). Among the various types of carbonaceous materials, most of the works were focused on activated carbon (AC).The thermal methane decomposition:

$$CH_4 \rightarrow C + 2H_2 \qquad \text{……..(1)}$$

is a simple, slightly endothermic reaction. Catalysts are needed to reduce the operation temperature.

In contrast to the ACs, which showed acceptable initial reaction rates but rapidly deactivated due to blocking of AC pores by growing crystallites which hinder the internal diffusion of methane molecules, most of the carbon surface is relatively easily accessible to methane molecules during decomposition reaction carbons differ in particle size, average aggregate mass, morphology, etc., for example, the oil furnace process produces carbons with particle diameters in the range 10–250 nm, and surface area of 25–1500m^2 g^{-1}. It was reported that the catalytic activity of different carbon samples remained almost unchanged despite a significant decrease in the surface area taking place during the reaction. In deactivation study of carbon, La´zaro et al (La´zaro et al.,2008) showed that the amount of surface complexes desorbed as CO, as well as the surface area, decreased gradually during the stable period of activity observed for the catalyst. In addition, it was found that the total pore volume decreased as the carbon is deposited and the degree of graphitization increased as the reaction progressed. In kinetic and deactivation study of carbon catalysts, Serrano et al. (Serrano et al 2009) showed that the most active catalyst at short reaction times was AC, but it underwent a fast deactivation due to the deposition of carbon from TCD of methane. During the methane TCD process, the catalyst deactivates due to intensive carbon deposition. The deposit normally has lower surface area and activity compared to the original carbon catalyst and its activity is influenced by its structure ranging from amorphous to crystalline depending on the way the carbon is formed. The order of catalytic activity of carbons according to its structure correlates with the following sequence: amorphous > turbostratic > graphite.

Additionally, the carbon produced might be a high added value product that could be used in multiple applications, such as building and construction materials, electricity production by direct carbon fuel cells, soil amendment and environmental remediation (Muradov and Veziroglu, 2005). The interesting feature of using carbonaceous catalysts: (1) the methane decomposition reaction can be catalyzed by carbon produced in the process, so an external catalyst would not be required (except for the start-up operation); and (2) the separation of carbon product from the carbon catalyst is not necessary (Hazzim et al, 2010).

In this study, the apparent kinetics of methane TCD and the deactivation kinetic of catalyst were studied using different reactant residence times

at 900 ◦C using AC manufactured from hardwood as a catalyst in a fixed bed operating mode. In addition, the study also examined the change in internal diffusion with time on-stream using Thiele modulus. The characterization of fresh and deactivated AC was also carried out under different operating conditions.

DEACTIVATION OF ACS

The activity of AC (a) is defined as:

$$a = \frac{R_t}{R_o} \qquad \text{……..(2)}$$

R_t: rate at which the pellet converts reactant
R_o: rate of reaction of A with a fresh pellet
and in terms of the fluid bathing the pellet the rate of reaction of A should be of the following form:
(reaction rate) =f_1(main stream temperature).f_3(main stream concentration). f_5 (present activity of the catalyst pellet) …….. (3)
Similarly, the rate at which the catalyst pellet deactivates may be written as:
(deactivation rate) = f_2(main stream temperature).f_4(main stream concentration). f_6(present state of the catalyst pellet) ……. (4)

In terms of nth-order kinetics, Arrhenius temperature dependency, and isothermal conditions, eq. (3) becomes, for the main reaction:

$$-r_A = k'.C_A^n.a = k'_o e^{-E/RT}.C_A^n.a \qquad \text{…. ……(5)}$$

and for deactivation which in general is dependent on the concentration of gas phase species, Eq. (4) becomes

$$-\frac{da}{dt} = k_d.C_i^m.a^d = k_{do} e^{-E_d/RT}.C_i^m.a^d \qquad \text{……(6)}$$

Where d is called the order of deactivation, m measures the concentration dependency and E_d is the activation energy or temperature dependency of the deactivation.
Thus as known from literature the rate of mass gain increases with temperature and gas hourly space velocity (GHSV) and higher temperature and GHSV used the faster the AC reaches the maximum amount of carbon that it can accumulate. In term of Arrhenius temperature dependency and for the deactivation rate which in general depends on methane density (ρ_{CH_4}) ; equation (6) becomes:

$$\frac{da}{dt} = k_d.\left(\frac{\rho_{CH_4}}{16}\right)^m.a^d = k_{do} e^{-E/RT}\left(\frac{\rho_{CH_4}}{16}\right)^m.a^d \qquad \text{……(7)}$$

where d is the order of the deactivation, k_d is the catalyst deactivation rate constant in(gmol .L^{-1}.min)$^{-1}$, m is a measure of the ρ_{CH_4} dependency, E_d is the activation energy or temperature dependency of the deactivation and k_{do} is the pre-exponential factor in (gmol .L^{-1}.min)$^{-1}$. The method of searching for a deactivation equation is analogous to that of homogeneous reaction where it starts with the simplest kinetic form and then evaluates if it fits the data.
Inserting the rate of Eq. (7) into the performance expression for mixed flow and applying the first first-order reaction and first-order deactivation which, in addition, is concentration independent gives:

$$\tau' = \frac{WC_{Ao}}{F_{Ao}} = \frac{W}{\upsilon} = \frac{C_{Ao} - C_A}{k'aC_A} \qquad \text{……..…(8)}$$

For steady flow in a mixed reactor we have found:

$$\ln \tau' = k_d t + \ln \frac{C_{Ao} - C_A}{k'C_A} \qquad \text{……..…(9)}$$

Figure (1) shows how to test for the kinetic expressions of Eq. (6) by this procedure. Actually there is no particular advantage in using varying flow over constant flow when testing for the kinetics of Eq. (6) or any other independent deactivation. However, for other deactivation kinetics the present reactor system is by far the most useful because it allows us to decouple the three factors C, *T,* and a and study them a pair at a time (Levenspiel , 1999).
If it does no fit first order kinetic, try another kinetic form and so on. Initially, equation (6) was integrated for different values of temperature and ρ_{CH_4} and then various equation forms (d = 0, 0.5, 1, 1.5 and 2) were tried for an integrated equation. The highest correlation coefficient (R^2) will be examined for each trial.

MECHANISM OF REACTION AND REACTION RATE EXPRESSION

Experimental observations of the present study indicate that the reaction is elementary. However the reaction mechanism and the identification of rate-controlling steps were attempted in the present study following the mechanism proposed by Snoeck et al. (Snoeck et al., 1997).They proposed the following mechanism for methane decomposition:

$$CH_4 + S \xleftrightarrow{k^{+1}} CH_4.S \qquad \text{……..…(10)}$$

$$CH_4.S + S \underset{k_{-2}}{\overset{k_{+2}}{\longleftrightarrow}} CH_3.S + H.S \quad \text{……..(11)}$$

$$CH_3.S + S \quad \text{……..…….…(12)}$$

$$CH_2.S + S \underset{k_{-4}}{\overset{k_{+4}}{\longleftrightarrow}} CH.S + H.S \quad \text{…..….(13)}$$

$$S \underset{k_{-5}}{\overset{k_{+5}}{\longleftrightarrow}} C.S + H.S \quad \text{…….....…..(14)}$$

$$C.S \underset{k_{-6}}{\overset{k_{+6}}{\longleftrightarrow}} C_C + S \quad \text{…….....….(15)}$$

$$2H.S \underset{k_{-7}}{\overset{k_{+7}}{\longleftrightarrow}} H_2 + 2S \quad \text{…….….(16)}$$

Whereas eq (11) represents the adsorption of methane on the surface of the catalyst, eqs (11) - (14) represent the surface reaction to form adsorbed methyl radicals and adsorbed hydrogen atoms on the catalyst surface. Equations (15) and (16) represent the deposition of carbon on the catalyst surface and desorption of hydrogen from the catalyst surface, respectively.

The performance equations for this rate form and mixed flow are analogous to those for plug flow, shown by Levinspil (Levinspil, 1999)

In diffusion-free regime

$$= \frac{C_{Ao}}{C_A} - 1 = k'.\tau.a = k'.\tau.e^{-kd.t} \quad \text{.....(18)}$$

In strong diffusion regime

$$= \frac{C_{Ao}}{C_A} - 1 = k'.\tau.a\zeta = k'.\tau.e^{-kd.t}.\zeta \quad \text{…….....(19)}$$

If this rate form is correct then for both strong or no diffusion resistance effects a plot of ln $\left(\frac{CAo}{CA} - 1\right)$ vs t should give a straight line. Making this tabulation and plot, as shown in figure (5) shows that the above rate form fits the data. Hence, the guessed rate form fits the data.

Let us next see whether the reactor is operating in the diffusion-free or strong diffusion regime.

EXPERIMENTAL WORK

1. Materials

Hardwood activated carbon (C) manufactured by Norit Americas was used for TCD experiments. The as-received activated carbon was sieved, and particles between and 140 mesh (0.125 – 0.106 mm) are obtained. Methane (99.999%) from National Oxygen Pte Ltd and argon (99.999%) from Air Products were used without further purification.

2. Characterization methods

The analysis of surface area was used done on BET (Brunauer, Emmett, and Teller) and determined by an automated gas absorption analyzer, ASAP 2020 (Micromeritics, Instruments Inc., GA USA) and scanning electron microscopy (SEM) analysis of samples was performed by using a Phillips SEM-505 scanning electron microscope operated at 300 kV/SE and 50° inclination.

3. Reactor set-up

A fixed bed, quartez tubular reactor (50 mm OD, 48 mm ID, length of 150 mm) was used for methane decomposition (figure (2)). The product gas was sent to gas chromatography (GC) for analysis. Samples were automatically taken by GC every 10 minutes. The calibrations were performed using the reactor set-up by on-line injection of methane. 1.000 gm (dry base) of the activated carbon sample was weighed; the catalyst was placed inside the reactor on a small piece of glass wool on the screen at the bottom of the bed. The bed was not packed. Gas hourly space velocity (GHSV) of (6-20) l/hr.gm_{cat} was used with a small stream of argon used to heat the system to the experimental temperature in the heating system (furnace and coating).

Whereas eq (11) represents the adsorption of methane on the surface of the catalyst, eqs (11) - (14) represent the surface reaction to form adsorbed methyl radicals and adsorbed hydrogen atoms on the catalyst surface. Equations (15) and (16) represent the deposition of carbon on the catalyst surface and desorption of hydrogen from the catalyst surface, respectively.

RESULTS AND DISCUSSION

1. Rate of Decomposition and Deactivation

The growth of carbon deposit on the catalyst may follow a proposed mechanism which can be diagnosed by SEM image in figure (3) which supports that mechanism. Methane decomposes on the front surface of certain active sites of the carbon catalyst, and the carbon thus formed diffuses through the metal and precipitates at the rear surface. The driving force that pushes the carbon diffusion was suggested to originate from the concentration gradient of dissolved carbon between the two interfaces, i.e. the metal-gas

The result of examining the fitness of equation (9) due to the procedure mentioned earlier

is shown in figure (4), it shows that the correlation coefficient (R^2= 0.947) and k_d= -0.602. Thus equation (9) becomes:

$$\ln \tau' = -0.602t + \ln \frac{11.355 - C_A}{0.766 C_A} \quad \text{at 900 ◦C}$$

……..……..……(17)

Ed= 192 kJ/mol/l .The performance equations for this rate form and mixed flow are analogous to those for plug flow, shown by Levinspil (Levinspil, 1999)

In diffusion-free regime

$$= \frac{C_{Ao}}{C_A} - 1 = k'.\tau.a = k'.\tau.e^{-kd.t} \quad \text{.....(18)}$$

In strong diffusion regime

$$= \frac{C_{Ao}}{C_A} - 1 = k'.\tau.a\zeta = k'.\tau.e^{-kd.t}.\zeta \quad \text{……....(19)}$$

If this rate form is correct then for both strong or no diffusion resistance effects a plot of ln $\left(\frac{CAo}{CA} - 1\right)$ vs t should give a straight line. Making this tabulation and plot, as shown in figure (5) shows that the above rate form fits the data. Hence, the guessed rate form fits the data.

Let us next see whether the reactor is operating in the diffusion-free or strong diffusion regime.

Guess No Intrusion of Diffusional Resistances. Then from Eq. (1) we have:

$$\ln\left(\frac{C_{Ao}}{C_A} - 1\right) = \ln(k'.\tau.a) = \ln(k'.\tau) - k_d t \quad \text{.....(20)}$$

From figure (5):-

The intercept = 2.73, slope = -1.0978

Thus at 6 L/hr, k' = 2.44 L.gm_{cat}.min^{-1}, k_d = 2.73 min^{-1}

E= 205 205 kJ mol/1.

Now check the Thiele modulus to verify that we really are in the diffusion resistance free regime. Thus at t = 0

$$M_T = L\sqrt{\frac{k'''}{D_e}} = \frac{0.165*10^{-3}}{6}\sqrt{\frac{2.44*1672}{6.83*10^{-5}}} = 1.288$$

Then MT is larger than 0.4 and less than 4, hence this value of Thiele modulus represents a fair pore diffusional resistance.

2. Surface Properties Changes

Fresh and spent area was examined by nitrogen adsorption isotherms. The presence of microporosity is also detected while the main contribution to the BET surface area is due to the presence of mesoporosity. According to the BJH model, the AC sample possesses a wide pore size distribution in the mesopore range (10–60A°).

Regarding the surface area of the fresh catalysts, it was found that the surface area cannot be related neither to the initial reaction rate nor the quasi-steady state reaction rate. For example, the surface areas of the fresh and spent catalysts were 885 and 997.572 m^2/g respectively, the differences in the reaction rate in the quasi-steady state they were 0.36 mol/min-gcat for the fresh catalyst and 0.112 mol/min-gcat for the spent one. This result is consistent with other results published in the literature for ACs (Lee et al, 2004, Giorgos et al, 2011) in which similar initial surface area did not imply the same reaction rate.

However, no definitive trend can be derived. It is well known that the performance of activated carbon can be affected by the deposition of, or the mutual interactions with, carbonaceous species.

The SEM images of the morphological appearance of the virgin and deactivated AC at decomposition temperatures of 800 and 900 ◦C are shown in figures (6, a and b). Carbon deposit is clearly seen on the surfaces of deactivated AC in the form of irregular agglomerate and this deposit leads to the blockage of the pore mouths, thus causing deactivation of the AC. Additional tests were performed at 800◦C and it appears that using two decomposition temperatures had no effect on the type of produced carbon.

The carbon catalyst produced filamentous like carbon and it is similar to the one formed while methane decomposition is performed on metal supported catalysts as reported earlier (Ashok et al, 2007). The growth of filamentous carbon may be due to the presence of trace amounts of metal components such as K, Na and Fe in the ash of activated carbon **(**Bai. *et al*, 2006). Therefore, it is suggested that the type of carbon formed from decomposition of methane is depends on the type of activated carbon and operation conditions of reaction.

CONCLUSIONS

The results of the experiments of thermocatalytic decomposition of methane by using AC derived from hardwood as a catalyst in a quartz fixed bed reactor at temperatures of 800, 850, and 900◦C, and different methane residence times calculated based on changing the gas hourly space velocity at a constant ACS weight were used to evaluate the apparent kinetics and catalyst deactivation and effect. The apparent kinetics shows that the reaction

order is 1 and activation energy is 205 kJmol/1.A deactivation order of 0.45 and deactivation energy of approximately 192 kJ mo/1 were obtained and a simple model of catalyst activity for methane decomposition over ACS has been developed. The result of calculation of Thiele Modulus indicated that diffusional limitation increased with time on-stream and it attributed to the deposition of carbon produced from methane decomposition with a fair pore resistance. A comparison between fresh and used ACSs showed that methane decomposition over ACS occurs mainly in micropores.

REFERENCES

- Hazzim F. Abbas, W.M.A. Wan Daud, "Thermocatalytic decomposition of methane using palm shell based activated carbon: Kinetic and deactivation studies", Fuel Processing Technology, 90, (2009) 1167–1174.
- La´zaro MJ, Pinilla JL, Suelves I, Moliner R. "Study of the deactivation mechanism of carbon blacks used in methane decomposition". Int J Hydrogen Energy 2008;33:4104–11.
- Muradov N.Z, T.N. Veziro lu, "From hydrocarbon to hydrogen–carbon to hydrogen economy", International Journal of Hydrogen Energy 30 (2005) 225–237.
- Levenspiel O., Chemical Reaction Engineering, Wiley, New York, 1999.
- Snoeck. J. W.; FrornenL. G. F.: Fowles. M. Kinetic Study of the Carbon Filament Formation by Methane Cracking on Nickel Catalysls. .J. *Cala!.* 1997. 169.250.
- Hazzim F. Abbas*, W.M.A. Wan Daud, Hydrogen production by thermocatalytic decomposition of methane using a fixed bed activated carbon in a pilot scale unit: Apparent kinetic, deactivation and diffusional limitation studies Int J Hydrogen Energy, 35 (2010) 12268-12276.
- Serrano D.P., Botas A., Guil-Lo´pez R., P. Pizarro, G. Go´mez, "Methane catalytic decomposition over ordered mesoporous carbons: A promising route for hydrogen production", International Journal of hydrogen energy 35 (2010) 9788 – 9794.
- Lee EK, Lee SY, Han GY, Lee BK, Lee TJ, Jun JH, et al. Catalytic decomposition of methane over carbon blacks for CO_2-free hydrogen production. Carbon 2004;42:2641–8.
- Giorgos Patrianakos, Margaritis Kostoglou, Athanasios Konstandopoulos, "One-dimensional model of solar thermal reactors for the co-production of hydrogen and carbon black from methane decomposition", Int J Hydrogen Energy, 36 (2011) 189-202.
- Ashok J, Naveen Kumar S, Venugopal A, Durga Kumari V, Tripathi S, Subrahmanyam M." CO_x free hydrogen by methane decomposition over activated carbons". Catal Commun 2008;9(1):164–9.
- Bai Z, Chen H, Li W, Li B." Hydrogen production by methane decomposition over coal char". Int J Hydrogen Energy 2006;31 (7):899-905.

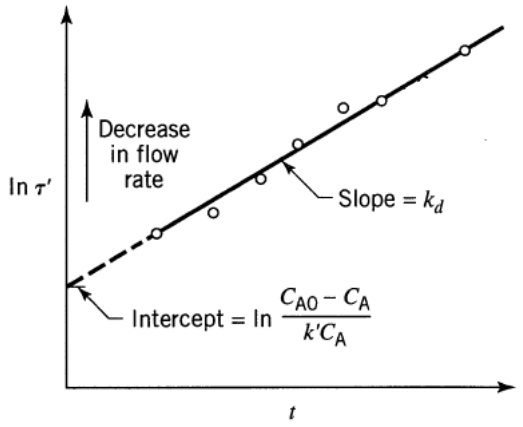

Figure (1) Test of the kinetic expressions of Eq. (5) using a batch of solids and changing flow of fluid in a mixed reactor so as to keep C_A constant (Levinspil, 1999)

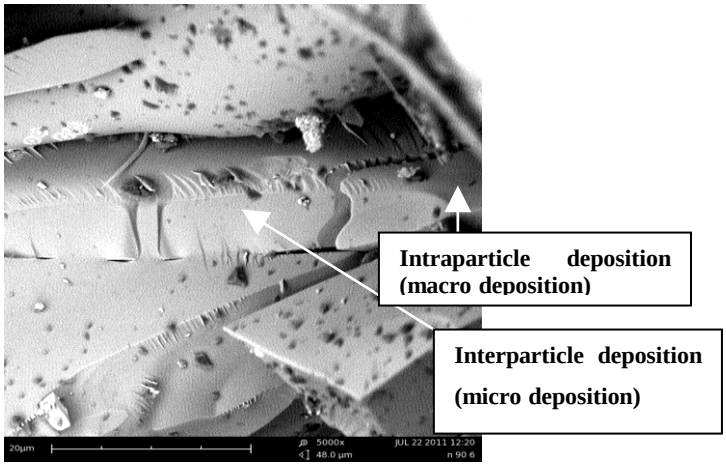

Figure. (3)Scanning electron microscope image of carbon formation (deposition) on the AC C particle.

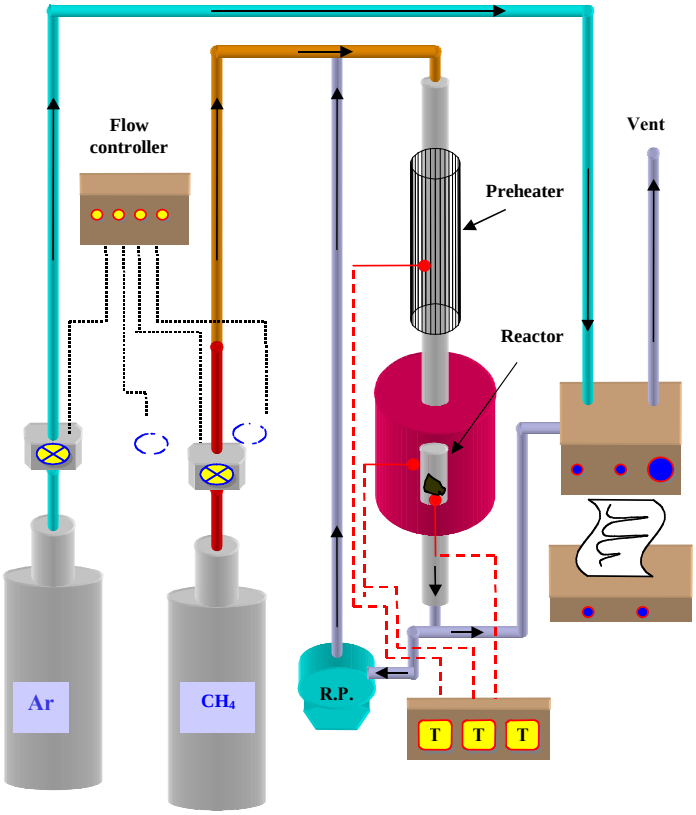

Figure (1): The schematic diagram of the experimental set-up for TCD

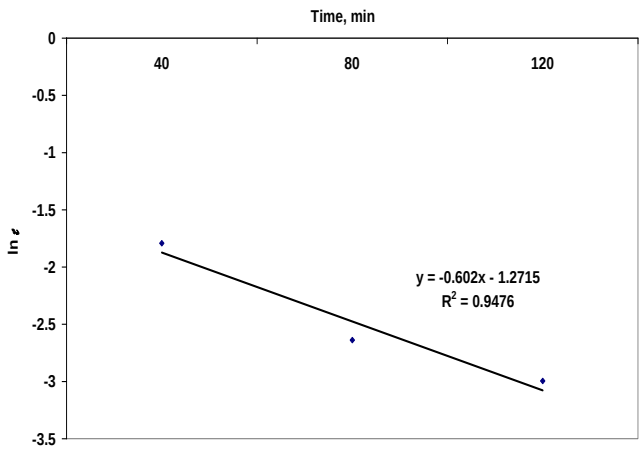

Figure (4). Test of the kinetic expressions of Eq. (19)

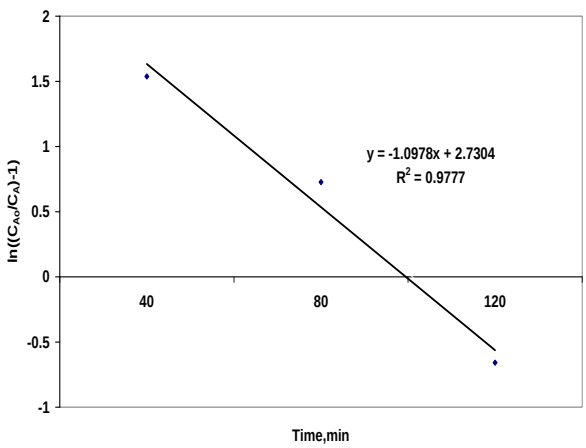

Figure (5 Fitting of rate data for AC C at 900 ◦C

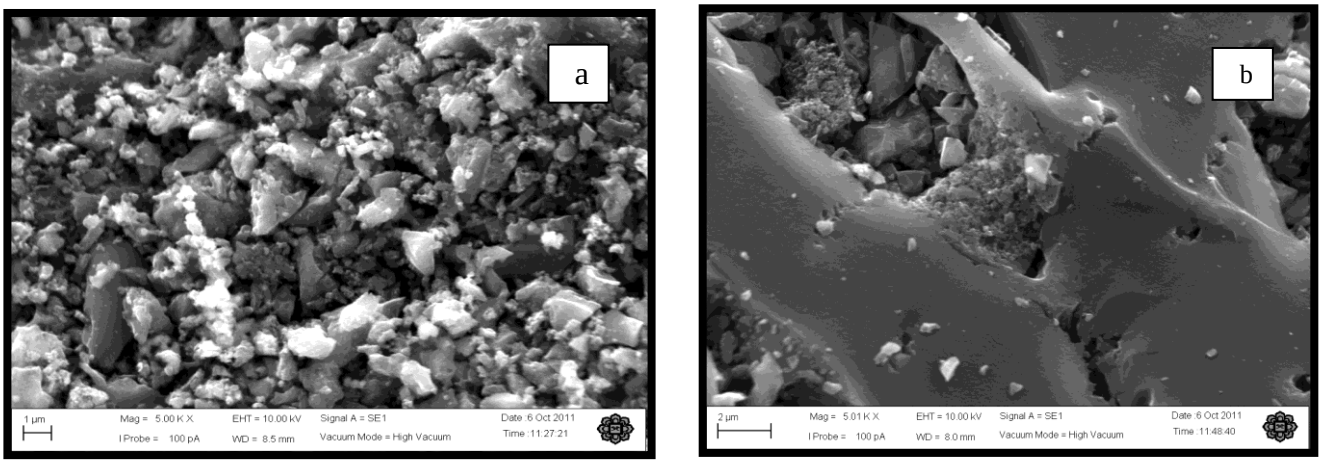

Figure (6) SEM images of AC surface: (a) virgin; (b) after decomposition at 900 ◦C.